JOC Article

# Advanced Oxidation Chemistry of Paracetamol. UV/$H_2O_2$-Induced Hydroxylation/Degradation Pathways and $^{15}$N-Aided Inventory of Nitrogenous Breakdown Products.

Davide Vogna,[†] Raffaele Marotta,[‡] Alessandra Napolitano,[†] and Marco d'Ischia*[,†]

*Department of Organic Chemistry and Biochemistry, University of Naples "Federico II", Via Cinthia 4, I-80126 Naples, Italy, and Department of Chemical Engineering, University of Naples "Federico II", Piazzale Tecchio, I-80126 Naples, Italy*

*dischia@cds.unina.it*

*Received February 8, 2002*

The advanced oxidation chemistry of the antipyretic drug paracetamol (**1**) with the UV/$H_2O_2$ system was investigated by an integrated methodology based on $^{15}$N-labeling and GC-MS, HPLC, and 2D $^1$H, $^{13}$C, and $^{15}$N NMR analysis. Main degradation pathways derived from three hydroxylation steps, leading to 1,4-hydroquinone/1,4-benzoquinone, 4-acetylaminocatechol and, to a much lesser extent, 4-acetylaminoresorcine. Oxidation of the primary aromatic intermediates, viz. 4-acetylaminocatechol, 1,4-hydroquinone, 1,4-benzoquinone, and 1,2,4-benzenetriol, resulted in a series of nitrogenous and non-nitrogenous degradation products. The former included *N*-acetylglyoxylamide, acetylaminomalonic acid, acetylaminohydroxymalonic acid, acetylaminomaleic acid, diastereoisomeric 2-acetylamino-3-hydroxybutanedioic acids, 2-acetylaminobutenedioic acid, 3-acetylamino-4-hydroxy-2-pentenedioic acid, and 2,4-dihydroxy-3-acetylamino-2-pentenedioic acid, as well as two muconic and hydroxymuconic acid derivatives. $^{15}$N NMR spectra revealed the accumulation since the early stages of substantial amounts of acetamide and oxalic acid monoamide. These results provide the first insight into the advanced oxidation chemistry of a 4-aminophenol derivative by the UV/$H_2O_2$ system, and highlight the investigative potential of integrated GC-MS/NMR methodologies based on $^{15}$N-labeling to track degradation pathways of nitrogenous species.

## Introduction

Advanced Oxidation Processes (AOP) comprise a range of water reclamation strategies aimed at achieving complete mineralization of organic pollutants to $CO_2$ and $H_2O$ by the action of highly reactive oxygen species generated by different techniques, including mainly photochemical systems (UV/$H_2O_2$, photoassisted Fenton, $TiO_2$-photocatalyzed, UV/$O_3$) and ozonation. [1−3]

Whereas the applications of AOP to recalcitrant aromatic pollutants have expanded dramatically in recent years, spurring extensive kinetic studies aimed at optimizing operational parameters, considerable lacunae remain as to the degradation mechanisms and the structures, origin, and fate of ring-opened acyclic products. Insights into this relatively unexplored segment of organic chemistry are hurdled by the need to contend with bewilderingly complex patterns of products at various degrees of oxygenation and degradation, often present as intimate mixtures of highly polar stereo- and regioisomeric species. Yet, pursuit of these issues is urged by the need to improve existing methodologies for the routine characterization of complex product mixtures in toto; to establish spectra libraries of degradation products for analytical purposes; and to verify the possible generation of toxic intermediates along the mineralization pathway more hazardous than the parent pollutants.

Among the various organic pollutants that are currently under scrutiny as substrates for AOP, phenolic compounds occupy a prominent position.[4−7] UV/$H_2O_2$ treatment of phenol was reported to give as main intermediates catechol, 1,4-hydroquinone, and a series of dimeric species, such as phenoxyphenols, which eventually decomposed to organic acids such as muconic, maleic, fumaric, D,L-malic, oxalic, and formic acid.[8,9] Salicylic acid behaved similarly to afford catechol and 2,3-dihydroxybenzoic acid, which in turn give rise to the same pattern of carboxylic acids as phenol.[8]

Photocatalytic degradation of 1,4-hydroquinone was found to yield a collection of oxocarboxylic acids via hydroxy-1,4-benzoquinone and 1,2,4-benzenetriol.[10]

[†] Department of Organic Chemistry and Biochemistry.
[‡] Department of Chemical Engineering.

(1) Andreozzi, R.; Caprio, V.; Insola, A.; Marotta, R. *Catal. Today* **1999**, *53*, 51−59.
(2) Pelizzetti, E.; Serpone, N. *Homogeneous and Heterogeneous Photocatalysis*; D. Reidel Publishing Company: Boston, 1986.
(3) Legrini, O.; Oliveros, E.; Braun, A. M. *Chem. Rev.* **1993**, 1446−1454.
(4) Andreozzi, R.; Marotta, R. *J. Hazard. Mater.* **1999**, *69*, 303−317.
(5) Esplugas, S.; Giménez, J.; Contreras, S.; Pascual, E.; Rodriguez, M. *Water Res.* **2002**, *36*, 1034−1042.
(6) Lunar, L.; Sicilia, D.; Rubio, S.; Perez-Bendito, D.; Nickel, U. *Water Res.* **2000**, *34*, 3400−3412.
(7) Andreozzi, R.; Caprio, V.; Insola, A.; Marotta, R. *Water Res.* **2000**, *34*, 463−472.
(8) Scheck, C. K.; Frimmel, F. H. *Water Res.* **1995**, *29*, 2346−2352.
(9) Huang, C. R.; Shu, H. Y. *J. Hazard. Mater.* **1995**, *41*, 47−67.

10.1021/jo025604v CCC: $22.00 
Published on Web 07/26/2002

The chemical steps in the photocatalytic degradation of 4-chlorophenol and 4-chlorocatechol have also been delineated and a number of aldehydes and oxocarboxylic acids have been identified, mainly by mass spectrometric analysis.[11]

Very little is known about the advanced oxidation chemistry of aminophenol derivatives.[6,12] Among these latter, paracetamol (acetaminophen, 4-acetylaminophenol, **1**), a widely used analgesic and antipyretic drug, and an important material for the manufacturing of azo dyes and photographic chemicals,[13] has recently attracted interest as a potential component of contaminated waters. Levels of **1** of up to 6 $\mu$g/L have been detected in effluent waters from sewage treatment plants.[14]

Because of its hepatotoxicity[15] and other side effects, concern has been raised about the possible environmental impact of **1** and its (bio)degradation products, which may be toxic or hazardous even in trace amounts.

Although the mode of polymerization of **1**, e.g. by the peroxidase/$H_2O_2$ system, is established, [16,17] the oxidative degradation pathways have remained a gap in the chemistry of **1**.

In this paper we report a survey of the advanced oxidation chemistry of **1** and related compounds with the UV/$H_2O_2$ system. By means of an integrated GC-MS and NMR approach based on $^{15}N$ labeling, it was possible to elucidate the competing hydroxylation/degradation pathways of **1** and to track specifically the fate of nitrogenous products.

## Results and Discussion

**Oxidation Conditions and Analytical Methods.** Advanced oxidation processes based on $H_2O_2$ with concomitant UV irradiation result in the production of OH radicals[18] and other reactive species that engage the organic pollutants to produce small hydrophilic species up to the level of inorganic materials (mineralization) innocuous to human health.[1−3] The system produces complete destruction of organic pollutants resistant to biological treatments, and is exploited for the cleanup of wastewaters because of chemical efficiency (high extent of mineralization) and practical convenience (low costs, ease of operation).[1] The aim of the present study was to identify as many products as possible and to dissect competing degradation pathways. To ease the analytical difficulties associated with the identification of nitrogenous species, $^{15}N$-labeled **1** was prepared by a straightforward route and was subjected to degradation under conditions identical with those used for the unlabeled drug. Product characterization was carried out by GC-MS and a combination of 2D $^{15}N$, $^{1}H$, and $^{13}C$ NMR techniques.

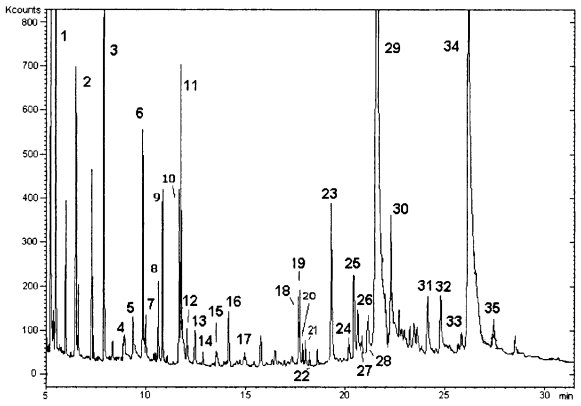


**FIGURE 1.** Representative GC trace for the UV/$H_2O_2$ degradation reaction of **1** as obtained at 20 min reaction time. Main carboxylic acids identified (as silyl derivatives): hydroxyacetic (glycolic) acid (1), oxalic acid (2), malonic acid (3), oxaloacetic acid (4), glyoxylic acid (5), maleic and fumaric acids (6 and 9), succinic acid (7), tartronic (hydroxymalonic) acid (11), ketomalonic acid (15), malic (hydroxysuccinic) acid (16), tartaric acids (19 and 23), α-ketoglutaric acid (22), and hydroxyketosuccinic acid (24). Structural formulations were secured by comparison of the chromatographic and mass spectrometric behavior of the products with those of authentic compounds or library matching exceeding 90%.

**Product Analysis: GC-MS.** In typical experiments, reaction of **1** (1 mM) or its $^{15}N$-labeled derivative was carried out with 100 mM $H_2O_2$ and UV radiation (254 nm) and GC-MS runs were performed at various intervals of time. A silylation treatment prior to injection into the gas chromatograph proved essential to allow for analysis of highly polar polyhydroxylated and carboxylated species. In all cases, complete silylation of both alcoholic and carboxylic functions was observed. Omission of the derivatization step resulted in chromatographic traces of poor analytical value.

About 50% consumption of **1** was observed after 20 min, and this was selected as a suitable reaction time for investigation of early intermediates and degradation products thereof. No substantial changes of product distribution were observed when the UV/$H_2O_2$ reaction was carried in phosphate buffer at pH values in the range 5.5−8.0 rather than in water.

Figure 1 shows a representative GC trace for the UV/$H_2O_2$ degradation reaction of **1** as obtained at 20 min reaction time.

The aromatic compounds that could be identified included, besides unreacted **1** (peak 29), 4-acetylaminocatechol (peak 34, the main component), 1,4-hydroquinone (peak 12), 1,2,4-benzenetriol (peak 21), 1,2,4,5-benzenetetraol (peak 27), and 4-acetylaminoresorcine (peak 32, identified by straightforward analysis of the EI-MS spectrum). In addition, a number of carboxylic acids could be identified (see legend to Figure 1). Sodium borohydride reduction of the mixture prior to analysis resulted in only minor differences in GC traces at various times. In particular, no appreciable change in 1,4-hydroquinone levels was observed after reduction.

Structural assignments for the main nitrogenous species, as deduced by ion trap MS data for both unlabeled and $^{15}N$-labeled **1**, are given in Table 1.

(10) Li, X.; Cubbage, J. W.; Tetzlaff, T. A.; Jenks, W. S. *J. Org. Chem.* **1999**, *64*, 8509−8524.
(11) Li, X.; Cubbage, J. W.; Jenks, W. S. *J. Org. Chem.* **1999**, *64*, 8525−8536.
(12) Andreozzi, R.; Caprio, V.; Insola, A.; Marotta, R. *Water Res.* **2000**, *34*, 463−472.
(13) Rao, E. K.; Sastry, C. S. *Mikrochim. Acta* **1984**, *1*, 313−19.
(14) Daughton, C. G.; Ternes, T. A. *Water Res.* **1998**, *32*, 3245−3260.
(15) O'Brien, P. J.; Khan, S.; Jatoe, S. D. *Adv. Exp. Med. Biol.* **1991**, *283*, 51−64.
(16) Potter, D. W.; Miller, D. W.; Hinson, J. A. *J. Biol. Chem.* **1985**, *260*, 12174−12180.
(17) Potter, D. W.; Hinson, J. A. *J. Biol. Chem.* **1987**, *262*, 966−973.
(18) Baxendale, J. H.; Wilson, J. A. *Trans. Faraday Soc.* **1957**, *53*, 344.

**TABLE 1. Main Nitrogenous Products in the Advanced Oxidation of [$^{15}$N]1 Identified by GC-MS Analysis.**

| *Peak #* ($t_R$, min) | Compound | F.W. | EI-MS: *m/z* values (relative abundance) | *Peak #.* ($t_R$, min) | Compound | F.W. | EI-MS: *m/z* values (relative abundance) |
|---|---|---|---|---|---|---|---|
| ***10*** (11.61) | 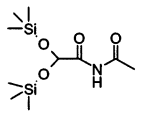 | 277 | 262(9), 220(39), 206(2), 191(100), 147(34), 130(12), 116(7), 103(5), 75(10), 73(50), 45(15), 43(20). $^{15}$**N:** 263(2), 221(45), 207(9), 191(90), 147(100), 131(23), 117(11), 103(13), 75(45), 73(85), 45(28), 43(29). | ***28*** (21.19) and ***30*** (22.39) | 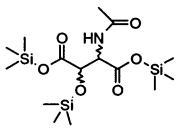 | 407 | 392(19), 350(6), 302(12), 261(64), 220(17), 189(30), 170(9), 147(88), 132(13), 116(14), 73(29). $^{15}$**N**: 393(34), 351(16), 303(29), 262(100), 220(32), 189(30),171(6), 147(64), 133(29), 117(30), 73(89) |
| ***14*** (12.49) | 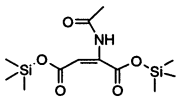 | 317 | 302(63), 275(28), 260(81), 212(44), 200(100), 184(17), 170(36), 158(18), 147(38), 130(12), 110(13), 98(7), 73(34). $^{15}$**N**: 303(68), 276(31), 261(97), 213(46), 201(100), 185(23), 171(37), 159(11), 147(48), 130(11), 111(14), 99(9), 73(38). | ***31*** (24.29) | 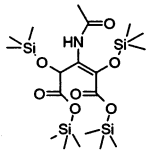 | 507 | 492(27), 450(25), 422(24), 390(29), 360(19), 348(89), 332(21), 305(12), 273(9), 260(20), 189(17),147(40), 73(100), 43(29). $^{15}$**N**: 493(32), 451(13), 423(21), 391(17), 361(18), 349(100), 333(23), 305(9), 274(8), 261(19), 189(24), 147(29), 73(100), 43(29). |
| ***17*** (14.91) | 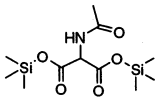 | 305 | 290(15), 261(45), 248(59), 246(38), 231(21), 220(59), 219(34), 204(15), 147(80), 132(45), 116(17), 102(15), 75(26), 73(100), 45(28), 43(38). $^{15}$**N**: 291(14), 262(44), 249(26), 247(49), 231(27), 221(45),220(44), 205(6), 147(92), 133(50), 117(22), 102(14) ,75(27), 73(100), 45(30), 43(45). | ***32*** (24.84) | 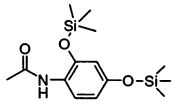 | 311 | 311(100), 296(9), 269(32), 254(10), 238(7), 206(21), 181(9), 166(14), 147(12), 73(53), 43(15). $^{15}$**N**:312(100), 297(32), 270(61), 255(23), 239(5), 207(31), 182(22), 167(7), 147(16), 73(46), 43(22). |
| ***18*** (17.61) | 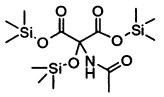 | 393 | 378(30), 336(12), 308(45), 276(62), 259(13), 246(38), 234(100), 218(8), 172(9), 147(55), 116(26), 73(72) $^{15}$**N**: 379(30), 337(18), 309(44), 277(65), 260(14), 247(43), 235(100), 219(14), 173(12),147(52), 117(28), 73(71) | ***33*** (25.95) | 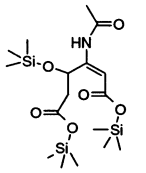 | 433 | 418(47), 376(23), 343(26), 328(44), 300(21), 258(18), 232(39), 202(11), 184(9), 147(42), 73(100), 43(27). $^{15}$**N**: 419(78), 377(38), 344(46), 329(66), 301(5), 259(37), 233(69), 202(34), 185(13), 147(76), 73(100), 43(78). |
| ***25*** (20.52) | 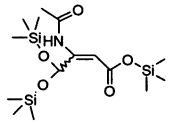 | 391 | 391(16), 376(42), 334(32), 302(32), 275(14), 260(38), 200(47), 184(14), 170(18), 147(62), 73(100). $^{15}$**N**: 392(1), 377(4), 335(5), 303(38), 276(22), 261(57), 201(100), 185(17), 171(23), 147(39), 73(41). | ***34*** (26.41) | 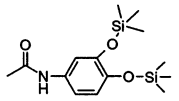 | 311 | 311(100), 296(8), 269(34), 254(13), 238(3), 206(19), 181(9), 166(1), 147(7), 73(50), 43(17). $^{15}$**N**: 312(100), 297(36), 270(52), 255(21), 239(6), 207(30), 182(19), 167(5), 147(15), 73(70), 43(21). |
| ***26*** (20.65) | 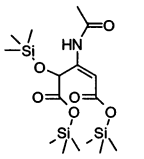 | 419 | 404(33), 362(28), 334(39), 318(5), 302(15), 260(42), 244(52), 217(8), 200(6), 184(12), 147(51), 73(100),43(42). $^{15}$**N**: 405(23), 363(18), 335(22), 319(19), 303(18), 261(100), 245(38), 217(18), 201(9), 185(14), 147(53), 73(56), 43(58). | ***35*** (27.37) | 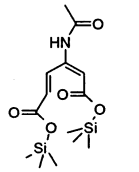 | 343 | 343(12), 328(8), 286(15), 269(21), 226(100), 206(19), 184(16), 136(65), 73(15), 43(14). $^{15}$**N**: 344(14), 329(6), 287(10), 270(32), 227(100), 207(24), 185(10), 137(70), 73(20), 43(18). |

Peak 10 was formulated as disilylated *N*-acetyl glyoxylamide hydrate on the basis of a $(M - 15)^+$ peak at *m/z* 262, a base peak at *m/z* 191[19] akin to that observed in the case of glyoxylic acid, and a fragmentation pattern reminiscent of that of glyoxylic acid (see Supporting Information).

The product eluted under the small peak at $t_R$ 12.49 min (peak 14) gave a meaningful fragmentation spectrum with an intense $(M - 15)^+$ peak at *m/z* 302, a base peak at *m/z* 200, denoting loss of COOTMS radical, and a peak at *m/z* 184, taken as diagnostic of the 3-acetylaminopropenoic acid moiety. It was thus assigned the structure of the disilyl derivative of acetylaminomaleic acid. Likewise, the product for peak 18, one of the most abundant intermediates along the degradation pathway, was identified as the trisilyl derivative of acetylaminohydroxymalonic acid, whereas peak 17 was regarded as being due to the disilyl derivative of acetylaminomalonic acid.

Peak 25 displayed a molecular ion peak at *m/z* 391, and significant fragmentation peaks at *m/z* 184 (vide supra) and at *m/z* 200 $(M - 191)^+$, denoting loss of the TMSO═C−OTMS radical, consistent with a derivative of 3-acetylamino-4,4-dihydroxy-2-butenoic acid (the hydrated form of 3-acetylamino-4-oxo-2-butenoic acid).

Two main nitrogen-containing products at the four-carbon level of degradation of the aromatic ring eluted as peaks 28 and 30, and were formulated as diastereoisomeric 2-acetylamino-3-hydroxybutanedioic acids. Strongly supportive of this assignment was a peak at *m/z* 189 characteristic of structures possessing a hydroxyacetic acid moiety.

Peak 26 was due to a species displaying a $(M - CH_3)^+$ fragment at *m/z* 404, another significant fragmentation peak at *m/z* 200 $(M - 219)^+$, suggesting direct loss of the TMSOCHCOOTMS radical from the molecular radical cation (*m/z* 419), and the fragment at *m/z* 184. Accordingly, it was assigned the structure of 3-*N*-acetylamino-4-hydroxy-2-pentenedioic acid.

(19) Spiteller, G.; Spiteller, S. *Biochim. Biophys. Acta* **1998**, *1392*, 23−40.

**TABLE 2. Selected Heteronuclear Correlation Data from 2D-NMR Experiments on Crude Mixtures Obtained by Oxidation of [$^{15}$N]1 and Proposed Structural Assignments.**

| compd no. | $^1$H | $^{15}$N | $^{13}$C | $^1$H−$^{15}$N HMBC | $^1$H−$^{13}$C HMBC | structure |
|---|---|---|---|---|---|---|
| **1** | 1.75 (s) | | 22.5 | 110.8 | 172.9 | acetamide[a] |
| | 6.63 (d, $J$ = 86 Hz) | 110.8 | | | 172.9 | |
| | 7.26 (d, $J$ = 86 Hz) | 110.8 | | | | |
| **2** | 7.74 (d, $J$ = 88 Hz) | 107.5 | | | 162.4 | oxalamide[a] |
| | 8.04 (d, $J$ = 88 Hz) | 107.5 | | | | |
| **3** | 1.95 (s) | | 23.9 | 133.6 | 167.7 | 4-acetylaminocatechol[a] |
| | 6.59 (d, $J$ = 8.4 Hz) | | 115.3 | | 133.6, 145.0 | |
| | 6.73 (m) | | 110.4 | 133.6 | 107.9, 141.2 | |
| | 7.11 (dd, $J$ = 2.0, 2.1 Hz) | | 107.9 | 133.6 | 141.2, 110.4 | |
| | 8.58 (s) | | | | | |
| | 8.94 (s) | | | | | |
| | 9.56 (d, $J$ = 88 Hz) | 133.6 | | | 141.2 | |
| **4** | 2.0 | | 24.5 | 132.5 | | 3-(acetylamino)−2,4-dihydroxy-2-pentenedioic acid |
| | 5.65 | | 78[c] | 132.5 | | |
| | 9.62 (d, $J$ = 88 Hz) | 132.5 | | | | |
| **5** | 4.51 | | 72.2 | 119.5 | 171.6 | 2-(acetylamino)−2,3-dihydroxybutanedioic acid |
| | 8.09 (d, $J$ = 88 Hz)[b] | 119.5 | | | | |
| **6** | 5.4 (m) | | 82[c] | | | acetylaminoglyoxylic acid |
| | 8.41 (d, $J$ = 88 Hz)[b] | 116.3 | | | | |

[a] Proton resonances were in good agreement with those of authentic samples. [b] Deduced from the COSY spectrum. [c] Deduced from HMQC.

By similar reasoning, the product eluted under peak 31, featuring a $(M - CH_3)^+$ peak at *m*/*z* 492, a fragment at *m*/*z* 273, conceivably via loss of the TMSOCHCOOTMS radical, a fragment at *m*/*z* 260 suggesting a silylated 2-hydroxy-3-acetylaminopropenoic acid moiety, and the peak at *m*/*z* 189, was formulated as deriving from 2,4-dihydroxy-3-acetylamino-2-pentenedioic acid.

The remaining two nitrogenous species eluted under the relatively retained peaks 35 and 33 were evidently ring-opened products of **1**. The former was assigned the structure of a muconic-type cleavage product, 3-*N*-acetylamino-2,4-hexadienedioic acid. The latter was apparently a hydroxylated derivative, exhibiting very intense nitrogen-containing fragmentation peaks at *m*/*z* 328, shared also by peak 35, and at *m*/*z* 232.

HPLC and GC-MS analysis of the oxidation mixtures after prolonged reaction times showed complete disappearance of primary intermediates and the almost exclusive presence of small fragments, e.g. acetic acid, oxalic acid, and formic acid with TOC values of about 80%. Formic acid from 1 mM **1** was less than 0.5 mM at 30 min reaction time and increased up to 1.15 mM after 80 min.

**Product Characterization: $^{15}$N, $^1$H, and $^{13}$C NMR.** Aliquots of reaction mixtures obtained by UV/$H_2O_2$ oxidation of $^{15}$N-labeled **1** were withdrawn at various intervals of time, carefully lyophilized, and subjected to $^{15}$N NMR analysis. At 50 min reaction time the spectrum revealed clusters of $^{15}$N resonances spread over the range between $\delta$ 100 and 170, suggesting significant modification of the chemical environment of the amide nitrogen ($\delta$ 133.0 for **1**). Proton signals showing well-discernible cross-peaks with the nitrogen resonances were then selected (Figure 2) and relevant homonuclear and heteronuclear one-bond and multiple-bond connectivities were deduced on the basis of $^1$H,$^1$H COSY, $^1$H,$^{13}$C HMQC, and $^1$H,$^{13}$C HMBC spectra. The main nitrogenous products identified under different reaction conditions by NMR analysis and the relevant $^1$H, $^{15}$N, and $^{13}$C chemical shift data are reported in Table 2.

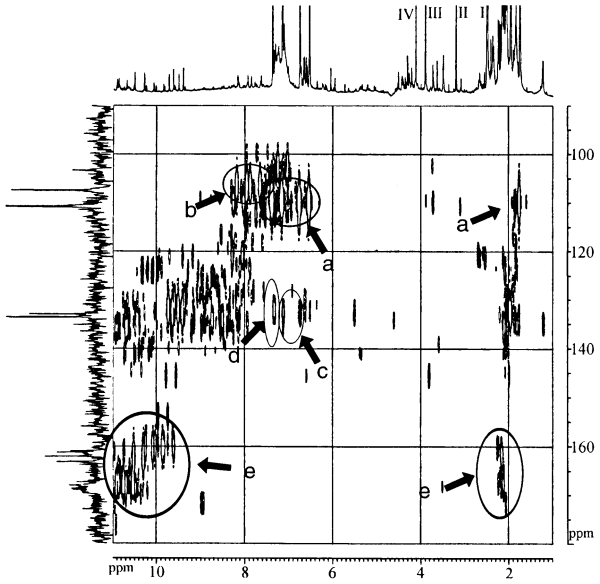


**FIGURE 2.** $^1$H,$^{15}$N HMBC NMR spectrum of the oxidation mixture of $^{15}$N-**1** at 50 min reaction time. Letters denote cross-peaks for identified species: a, acetamide; b, oxalic acid monoamide; c, 4-acetylaminocatechol; d, **1**; and e, imides. Numbers in the $^1$H NMR spectrum mark major non-nitrogenous compounds: I, succinic acid; II, malonic acid; III, glycolic acid; and IV, 2-oxo-3-hydroxybutanedioic acid.

Besides some residual **1**, 4-acetylaminocatechol appeared prominently in the early stages and gave well-recognizable $^1$H−$^{15}$N correlations (Figure 2, region c). A noticeable degradation product, which eluded GC-MS analysis, was acetamide giving an intense nitrogen signal at $\delta$ 110.8 correlating with two proton doublets at $\delta$ 6.63 and 7.26 (Figure 2, region a) due to the large $^1$H−$^{15}$N coupling constant and restricted rotation around the C−N bond.

Another nitrogen signal at $\delta$ 107.5 exhibited one-bond correlation with a pair of doublets at $\delta$ 7.74 and 8.04 (Figure 2, region b), suggesting an amide $NH_2$ group. An

appreciable long-range correlation of the doublet at $\delta$ 7.74 with a quaternary carbon signal at $\delta$ 162.4 and the lack of detectable cross-peaks in all other 2D correlation spectra, together with mechanistic considerations, suggested oxalic acid monoamide as a plausible candidate. This conclusion was corroborated by comparison of $^1$H and $^{13}$C NMR data with those of an authentic sample.

Two distinct clusters of nitrogen signals were apparent at $\delta$ 161−163 and 168−170, which displayed $^1J$ correlation with an array of doublets between $\delta$ 9 and 11 and long-range couplings with methyl signals around $\delta$ 2.2 (region e). These indicated N−H groupings experiencing a relatively deshielding environment. Such a feature was compatible with most of the ring breakdown structures deduced from GC-MS analysis, in which the NH group was linked to electron-withdrawing carboxyl-bearing residues such as imides. For comparison, a $\delta$ value of 186 was predicted for the $^{15}$N resonance of the 3D energy-minimized molecular structure of acetimide[20] as a model imide.

Main non-nitrogenous products identified by $^1$H,$^{13}$C one-bond and multiple-bond correlation were glycolic, malonic, succinic, and 2-oxo-3-hydroxybutanedioic acid (Figure 2, proton spectrum). Diastereoisomeric tartaric acids as well as malic, fumaric, and tartronic acid (hydroxymalonic acid), though supposedly present, could not be identified unambiguously because their $^1$H and $^{13}$C signals fell in exceedingly overcrowded spectral regions.

Both $^1$H and $^{13}$C NMR spectra ruled out the presence of significant levels of aldehyde products in the oxidation mixture, consistent with the GC-MS data. 1,4-Hydroquinone and 1,4-benzoquinone were also below detection limits.

**Oxidation Behavior of Reaction Intermediates.** To determine the origin of the various breakdown species identified in the mixture, established or putative aromatic intermediates, viz. 1,4-benzoquinone, 1,4-hydroquinone, 1,2,4-benzenetriol, and 4-acetylaminocatechol, as well as 4-aminophenol, were separately subjected to oxidation with the UV/$H_2O_2$ system under the same conditions.

The behavior of 1,4-benzoquinone toward the UV/$H_2O_2$ system is worthy of discussion. At 1 mM concentration, the compound was readily degraded in an oxygen-independent manner with partial conversion to 1,4-hydroquinone. The latter species attained maximum concentration (ca. 0.5 mM) after about 15 min and then decayed to trace levels after 40 min (Figure 3). GC-MS analysis indicated, besides 1,4-hydroquinone as the main product, small amounts of 1,2,4-benzenetriol, as well as of malonic, maleic, malic, succinic, fumaric, tartaric (both meso and D,L diastereoisomers), and 2-ketoglutaric acid. In the absence of $H_2O_2$, UV irradiation of 1,4-benzoquinone resulted in a similar decay as in the presence of $H_2O_2$, but under these latter conditions 1,4-hydroquinone accumulated up to a concentration of ca. 0.5 mM (50% yield) without substantial decomposition over 60 min. By contrast, negligible 1,4-benzoquinone decay was observed by exposure to $H_2O_2$ in the absence of UV radiation.

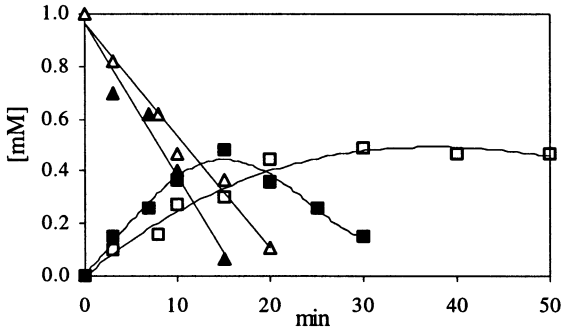


**FIGURE 3.** UV light irradiation of 1,4-benzoquinone in the presence or in the absence of hydrogen peroxide. 1,4-Benzoquinone (Δ) decay and 1,4-hydroquinone (□) formation by UV light. 1,4-Benzoquinone (▲) decay and 1,4-hydroquinone (■) formation by UV/$H_2O_2$ system.

**SCHEME 1**

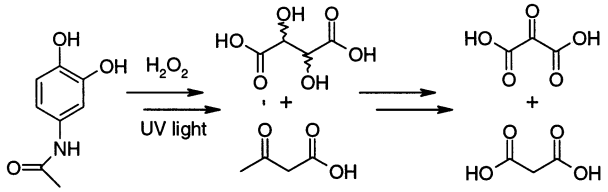


1,4-Hydroquinone gave mainly malonic acid, 1,2,4-benzenetriol, tartaric acids, and 1,2,4,5-benzenetetraol, whereas 1,2,4-benzenetriol afforded initially 1,2,4,5-benzenetetraol and then malonic acid, tartronic acid, malic acid, and tartaric acids.

4-Acetylaminocatechol gave mainly malonic, 3-oxobutanoic, tartronic, and tartaric acid (Scheme 1). At 1 mM concentration, 4-aminophenol disappeared in about 30 min giving rise to some 1,4-hydroquinone, but no detectable 1,2,4-benzenetriol, and a range of non-nitrogenous fragments. A remarkable feature of the GC trace was a group of products eluted at higher retention times than 4-aminophenol, sharing molecular ion peaks at *m*/*z* 642, or $(M - 15)^+$ peaks at *m*/*z* 627. Their mass spectra were strongly reminiscent of that of mucic acid (galactaric acid), which, however, was absent in the mixture. These species were tentatively formulated as isomeric tetrahydroxyhexanedioic acids and were not investigated further.

**Mechanistic Issues.** There is general consensus that UV/$H_2O_2$-promoted oxidations involve mainly OH radicals produced by photolysis of $H_2O_2$.[18] However, the actual situation may be much more complex, due to several concurrent oxidation pathways, e.g. reaction of $H_2O_2$ with excited states of the substrate and intermediates, the intervention of (hydro)peroxyl radicals, and so forth. In fact, under the experimental conditions adopted in this study UV absorption by $H_2O_2$ is not sufficient to rule out direct photolysis and other OH radical-independent photochemical processes.[21]

Moreover a significant role for atmospheric oxygen was ruled out by control experiments carried out under an argon atmosphere, giving similar product patterns. *tert*-

(20) A value of $\delta$ 186 ppm was predicted for the $^{15}$N resonance of $(CH_3CO)_2NH$. The experimentally measured $^{15}$N chemical shift value of acetamide was used for estimation of the expected resonances.

(21) $\epsilon_{254nm}$(**1**) = 7420 $M^{-1}$ $cm^{-1}$, $\epsilon_{254nm}(H_2O_2)$ = 18.6 $M^{-1}$ $cm^{-1}$, absorbed fraction $(H_2O_2) = \epsilon_{254nm}(H_2O_2) \times [H_2O_2]/(\epsilon_{254nm}(H_2O_2) \times [H_2O_2] + \epsilon_{254nm}(\mathbf{1}) \times [\mathbf{1}]) = 0.20$.

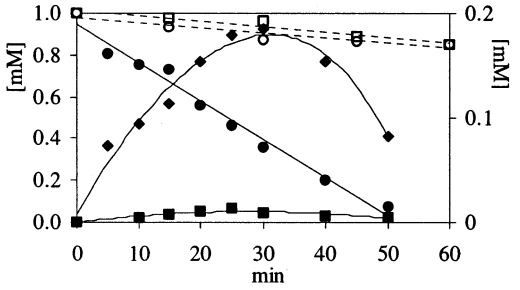


**FIGURE 4.** Time course of the decay of **1** and formation of 4-acetylaminocatechol and 1,4-hydroquinone by reaction with the UV/$H_2O_2$ system. Left axis: solid line, decay of **1** (●); dashed lines, experiments in the presence of 100 (□) or 200 mM (○) *tert*-butyl alcohol. Right axis: 4-acetylaminocatechol (♦) and 1,4-hydroquinone (■).

**SCHEME 2**

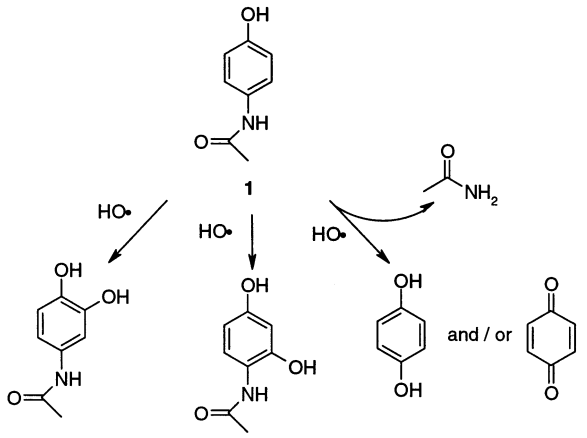


Butanol, an established OH radical scavenger,[22] decreased the rate of decay of **1** in a concentration-dependent manner (Figure 4). UV or $H_2O_2$, separately, induced little or no degradation of **1**. These findings indicated that OH radicals actually play a major role in the oxidative degradation of **1** and other phenolic species, e.g. 1,4-hydroquinone, and that direct photolysis is of minor importance. By contrast, direct photolysis may become an important contributory factor in the degradation of 1,4-benzoquinone and other quinonoid products in the mixture. The formation of 1,4-hydroquinone by photolysis of 1,4-benzoquinone without reductive treatment has already been reported in the literature.[10]

The structures of the early aromatic products indicated that three initial hydroxylation/oxygenation reactions compete as the initial step in the degradation of **1** (Scheme 2). These reactions would involve attack of the OH radical onto the aromatic ring of **1** leading to ortho, meta, and para hydroxylation with respect to the OH group.[1]H NMR monitoring of the reaction course in the very early stages (keeping substrate consumption below 20%) indicated a formation ratio of acetamide/4-acetylaminocatechol of ca. 1:1. In the reasonable assumption that nearly all of the acetamide initially formed derives from direct hydroxylation of **1**, it could be concluded that hydroxylation at the positions ortho and para (meta hydroxylation is of minor relevance) proceed to comparable degrees.

(22) Stoeffler, B.; Luft, G. *Chem. Eng. Technol.* **1998**, *70*, 1556−1559.

**SCHEME 3**

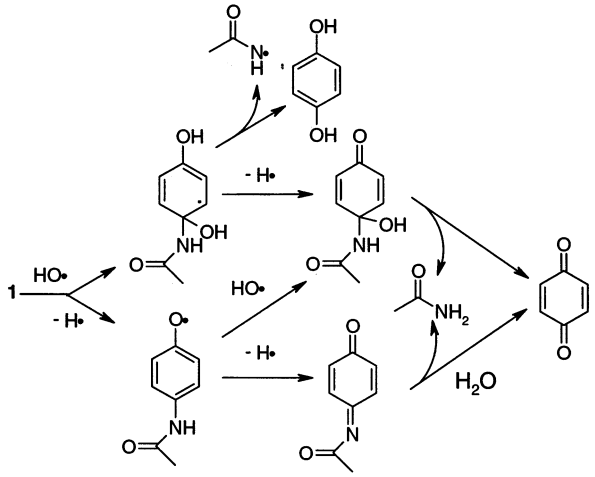


**SCHEME 4**

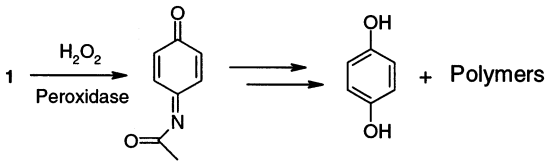


Different mechanistic options can be envisaged for OH radical-dependent para hydroxylation (Scheme 3). One would involve a direct substitution reaction to give 1,4-hydroquinone, by a mechanism similar to that reported for salicylic acid,[8] 4-hydroxybenzoic acid,[23] or 4-chlorophenol.[11] The other pathway would envisage conversion of the primary radical adduct to 4-acetylamino-4-hydroxy-2,5-cyclohexadienone, which would decompose to yield 1,4-benzoquinone and acetamide.

In the third pathway (Scheme 3), oxidation of **1** may proceed via H-atom abstraction leading to the semiquinone-like phenoxyl radical of **1**, which would then react with an OH radical or another oxygen species at the para position. Alternatively, further oxidation of the phenoxyl radical might lead to the corresponding quinoneimine, which could be susceptible to hydrolysis to generate 1,4-benzoquinone. Typically, however, H-abstraction from a phenoxyl OH is 1−3 orders slower than OH radical addition pathways and should contribute very little to the product pattern.

To probe the quinoneimine path, recourse was made to the peroxidase/$H_2O_2$ oxidation system, which produces the quinoneimine of **1** in the presence of excess $H_2O_2$ by a mechanism independent of OH radical formation. Oxidation of **1** (1 mM) with $H_2O_2$ (100 mM) in the presence of horseradish peroxidase resulted in a fast substrate consumption (90% within 1 min) leading to only small amounts of 1,4-hydroquinone, but no 4-acetylaminocatechol, 4-acetylaminoresorcine, and 1,4-benzoquinone (Scheme 4).

Little or no fragmentation products were observed, oligomeric and polymeric materials being the main products. TOC values were near 100%, thus confirming the lack of significant mineralization. This finding ruled out UV-independent hydroxylation/degradation of the

(23) Matsuura, T.; Omura, K. *Synthesis* **1977**, 173−184.

**SCHEME 5**

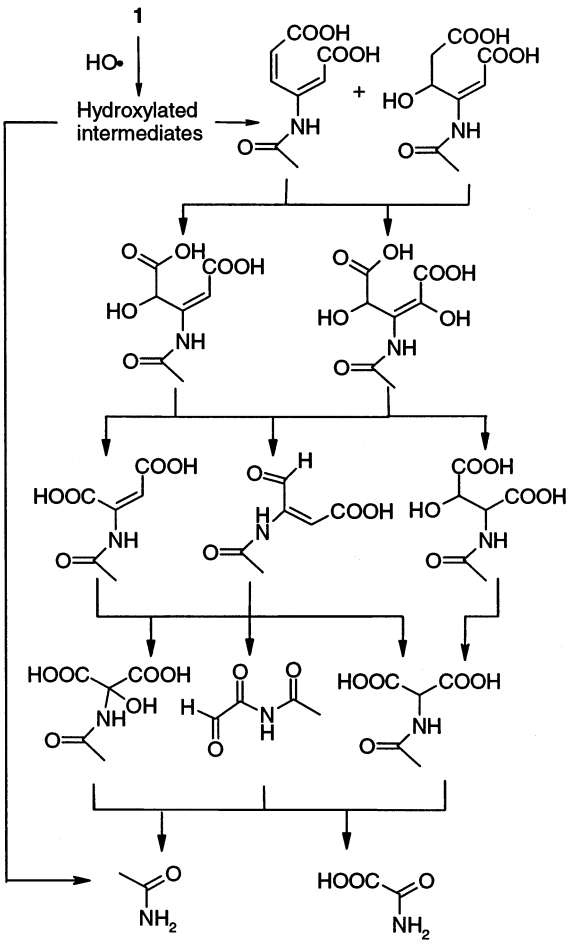


quinoneimine as a main reaction path of **1**. Nonetheless, the quinoneimine route may at least in part contribute to 1,4-benzoquinone/1,4-hydroquinone formation.

To assess the relative importance of degradation pathways downstream of the primary hydroxylation steps, competition experiments were performed in which 4-acetylaminocatechol and 1,4-hydroquinone or 4-acetylaminocatechol and 1,4-benzoquinone, with each component at 0.5 mM concentration, were exposed to UV/$H_2O_2$ in the same mixture (Figure 5).

The results indicated a remarkable susceptibility to oxidation of 1,4-benzoquinone, much greater than that

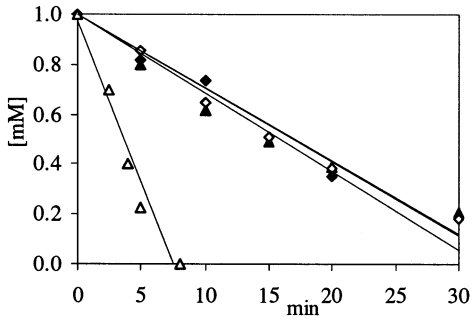


**FIGURE 5.** Decay of 4-*N*-acetylaminocatechol in the presence of 1,4-benzoquinone or 1,4-hydroquinone by reaction with the UV/$H_2O_2$ system: 4-*N*-acetylaminocatechol (▲) vs 1,4-benzoquinone and (Δ) 4-*N*-acetylaminocatechol (♦) vs 1,4-hydroquinone (◊).

of 1,4-hydroquinone and 4-acetylaminocatechol. This could explain why no significant levels of benzoquinone were detectable by HPLC during degradation of **1**. In control experiments, 1,4-benzoquinone did not oxidize **1** or 4-acetylaminocatechol by direct redox reaction. Plausible degradation pathways leading to nitrogenous breakdown products are sketched in Scheme 5. Such pathways are merely indicative and are not intended to provide a complete representation of the actual complexities of the degradation process. OH radicals, because of their proclivity for electron-rich aromatic compounds, could be mainly engaged with the hydroxylation of phenolic species, rather than of acyclic breakdown products, e.g. carboxylic acids. 1,4-Hydroquinone (via 1,4-benzoquinone), 4-acetylaminocatechol, and 4-acetylaminoresorcine would suffer further hydroxylation and/or one-electron oxidation by OH radicals to give semiquinones and, hence, quinones by disproportionation. These latter would undergo muconic-type cleavage, and in part also extradiolic cleavage, by the large excess of $H_2O_2$ through a UV-assisted mechanism.[24] The lack of detectable 4-aminophenol in the mixtures indicated that deacetylation is not a prominent route.

Oxalic acid monoamide, which accumulates together with acetamide during the early stages of the degradation of **1**, could in principle arise by sequential OH radical-induced hydroxylation steps of acetamide. However, exposure of pure acetamide to the UV/$H_2O_2$ system led to the formation of only negligible amounts of oxalic acid monoamide (NMR evidence), thus ruling out a substantial contribution of this route.

## Conclusions

This paper provides the first detailed inventory of intermediates and breakdown products formed by advanced oxidation of an aminophenol derivative. Besides the practical implications of the research, these results hold basic interest, as they expand the current knowledge of the oxidation chemistry of **1**, dissecting competitive hydroxylation routes and the structural factors determining the final outcomes. Additional interest stems from the potential of the combined GC-MS/NMR approach based on $^{15}N$ labeling to analyze nitrogenous degradation products. The detection by $^{15}N$ NMR of acetamide as a main degradation product eluding GC-MS analysis is paradigmatic in this regard. Finally, the generation of relatively low amounts of aldehydes and carbonyl products by degradation of 1,4-hydroquinone and 1,2,4-benzenetriol with the UV/$H_2O_2$ system compared to other systems[10] might be considered in assessing the ecological relevance of the present study.

## Experimental Section

**Materials.** Paracetamol (**1**), glycolic acid, glyoxylic acid, oxalic acid, oxalic acid monoamide, acetamide, 3-hydroxypyruvic acid, malonic acid, tartronic acid, ketomalonic acid, succinic acid, maleic acid, fumaric acid, malic acid, oxalacetic acid, D,L-tartaric acid, 2-ketoglutaric acid, mucic acid, 1,4-hydroquinone, 1,4-benzoquinone, 1,2,4-benzenetriol, *p*-aminophenol, 4-nitrocatechol, phenol, 1,1,1,3,3,3-hexamethyldisilazane (HMDS), chlorotrimethylsilane (TMSCl), and 30% hydrogen peroxide (w/

(24) Sawaky, Y.; Foote, C. S. *J. Am. Chem. Soc.* **1983**, *105*, 5035−5040.

w) were obtained from commercial sources and used as obtained. 1,2,4,5-Benzenetetraol was prepared by reduction of 2,5-dihydroxy-1,4-benzoquinone with sodium hyposulfite according to a reported procedure.[25] All other chemicals were of the highest grade commercially available. Doubly glass-distilled water was used throughout this study. Horseradish peroxidase (donor: $H_2O_2$ oxidoreductase, EC 1.11.1.7) type II (167 U/mg, RZ $E_{430}/E_{275} = 2.0$), bovine liver catalase ($H_2O_2$ oxidoreductase, EC 1.11.1.6), and [$^{15}$N]$NaNO_2$ (>99%) were used.

**Methods.** $^1$H, $^{13}$C, and $^{15}$N NMR spectra were recorded at 400.1, 100.6, and 40.5 MHz, in that order. An instrument fitted with a 5 mm $^1$H/broadband gradient probe with inverse geometry was used. For $^{15}$N NMR experiments delay values up to 10 s were used. Experiments used were standard Bruker implementations of gradient-selected versions of inverse ($^1$H detected) heteronuclear multiple quantum coherence (HMQC) and heteronuclear multiple bond correlation (HMBC) experiments. The HMBC experiments used a 100 ms long-range coupling delay. $^{15}$N chemical shifts were referenced to [$^{15}$N]-urea in DMSO-$d_6$ at $\delta$ 76.97 ppm, relative to $NH_3$ (liquid, 298 K) at 0.0 ppm ($^{15}$N NMR).[26] DMSO-$d_6$ was used as solvent.

TOC determinations were performed with a total organic carbon analyzer. Irradiation experiments were carried out in an annular reactor (420 mL) thermostated at 25 °C equipped with a 17 W low-pressure mercury monochromatic lamp (254 nm).

Calculations of chemical shift values were carried out on energy-minimized molecular structures with a Gaussian 01 program.[27]

**HPLC Analyses.** Analytical HPLC was carried out with an instrument equipped with a diode array detector. 0.1 M formic acid pH 3/$CH_3CN$ (95:5 v/v) was used as the eluant for determination of **1**, 1,4-benzoquinone, 1,4-hydroquinone, and 4-acetylaminocatechol with use of an octylsilane coated column (4.6 × 250 mm, 5 $\mu$m particle size) and a flow rate of 0.7 mL/min. Identification of reaction products was made by comparison of the chromatographic behavior (detection wavelength 254 and 280 nm) and UV spectra with those authentic samples. Quantitation was carried out by comparing integrated peak areas with external calibration curves.

For determination of formic acid, acetic acid, and oxalic acid, aliquots of the oxidation mixture of **1** (1 mL) were periodically withdrawn and added in a screw-capped vial to a solution (2 mL) of 1,2-phenylenediamine (22 mM) in 1% sulfuric acid. After being heated for 1 h at 100 °C, samples were neutralized with NaOH and analyzed by HPLC with use of a hexylsilane-coated column (2.0 × 25 mm, 10 $\mu$m particle size), with detection set at 254 nm. Phosphate buffer (0.1 M)/acetonitrile (90:10) containing 5% methanol was used as the mobile phase, at a flow rate of 0.5 mL/min.

**GC-MS Analyses**. GC-MS analyses were carried out on a GC instrument coupled with an ion trap detector using a 30 m cross-bond 5% diphenyl−95% dimethylpolysiloxane column (0.25 mm i.d., 0.25 $\mu$m df). Helium was the carrier gas with a 1 mL/min flow rate. Electron impact ionization was carried out at 70 eV. Data were processed with Saturn WS data analyses software. Temperature program: 80 °C, hold time 1 min; from 80 to 150 °C, rate = 7 °C/min; 150 °C, hold time 5 min; from 150 to 200 °C, rate = 7 °C/min; 200 °C, hold time 5 min. The inlet, transfer line, and manifold were taken at 250, 170, and 80 °C in that order. The acquisition started 4 min after the injection (solvent delay 4 min), and was set in scan mode in the range 40−650 amu. The threshold was fixed at 1 and sampling was 0.8 scans/s. For sample preparation 5-mL aliquots were taken at different times from the oxidation reaction of **1**, [$^{15}$N]**1**, 1,4-benzoquinone, 1,4-hydroquinone, 4-acetylaminocatechol, 1,2,4-benzenetriol, and 1,4-aminophenol, lyophilized, and treated with HMDS (200 $\mu$L), anhydrous pyridine (200 $\mu$L), and TMSCl (50 $\mu$L).[10] The resulting mixtures were shaken for 1 min and then centrifuged to separate the precipitate prior to injection into the chromatograph.

**Synthesis of [$^{15}$N]1**. To solution of phenol (488 mg, 5.3 mmol) and Na$^{15}NO_2$ (731 mg, 10.6 mmol) in water (25 mL) was added concentrated sulfuric acid (1 mL) under vigorous stirring in an ice-bath. After 15 min, the yellow precipitate formed was collected by filtration and dried. The solid thus obtained (659 mg) was treated with zinc powder (2.0 g) in glacial acetic acid (25 mL) and the mixture was taken under reflux for 1 h. After removal of solid materials, the mixture was taken to dryness under reduced pressure. The residue dissolved in 0.2 M carbonate buffer at pH 10 (30 mL) was treated with $Na_2S_2O_4$ (5 g) and, after 15 min, the mixture was filtered and added with acetic anhydride (2 mL). After 15 min, the mixture was extracted with ethyl acetate (3 × 20 mL) and the combined organic layers were washed with brine, dried over sodium sulfate, and taken to dryness. The residue (259 mg) was purified by silica gel column chromatography with chloroform/methanol 95:5 as the eluant to afford the title compound (180 mg, 22% yield) homogeneous to TLC (chloroform/methanol 90:10, $R_f$ 0.72). $^1$H NMR (DMSO-$d_6$), $\delta$ (ppm) 1.96 (s), 6.66 (d, $J$ = 8.0 Hz), 7.32 (dd, $J$ = 8.0, 1.6 Hz), 9.15 (s), 9.65 (d, $J$ = 88 Hz); $^{13}$C NMR (DMSO-$d_6$) $\delta$ (ppm) 23.8 ($CH_3$), 115.0 (CH), 120.0 (CH), 131.6 (C), 153.2 (C), 167.6 (C); $^{15}$N NMR (DMSO-$d_6$) $\delta$ (ppm) 133.0. GC-MS analysis (O-TMS derivative) $t_R$ 21.71 $m/z$ 224 ($M^+$, 100). [Found C, 63.09; H, 5.90; N, 9.88; $C_8H_9{}^{15}NO_2$ requires C, 63.14; H, 5.96; $^{15}$N 9.86.]

**Synthesis of 4-Acetylaminocatechol**. 4-Nitrocatechol (500 mg, 3.22 mmol) in 0.2 M carbonate buffer at pH 10 (40 mL) was added to $Na_2S_2O_4$ (5.6 g) at room temperature under stirring. After 15 min acetic anhydride (0.72 mL) was added and, after an additional 15 min, the mixture was extracted with ethyl acetate (3 × 30 mL). The combined organic layers were washed with brine, dried over sodium sulfate, and taken to dryness to afford the title compound as a colorless solid (480 mg, 89% yield) that was stored under vacuum to avoid darkening in air. $^1$H NMR (DMSO-$d_6$) $\delta$ (ppm) 1.95 (s), 6.59 (d, $J$ = 8.4 Hz), 6.73 (dd, $J$ = 8.4, 2.0 Hz), 7.11 (d, $J$ = 2.0 Hz), 8.58 (s), 8.94 (s), 9.56 (s); $^{13}$C NMR (DMSO-$d_6$) $\delta$ (ppm) 23.9 ($CH_3$), 107.9 (CH), 110.4 (CH), 115.3 (CH), 131.6 (C), 141.2 (C), 145.0 (C), 167.7 (C); GC-MS analysis (O-TMS derivative) $t_R$ 26.41 $m/z$ 311 ($M^+$, 100). [Found C, 57.51; H, 5.37; N, 8.42; $C_8H_9NO_3$ requires C, 57.48; H, 5.43; N, 8.38.]

**Oxidation Reaction: General Procedure**. Solutions of the appropriate substrate (1.0 mM) and hydrogen peroxide (100 mM) in water (420 mL) or 0.1 M phosphate buffer, pH 5.5, 7.0, or 8.0, were irradiated under stirring. Aliquots of the mixture were taken periodically and subjected to analysis (HPLC, GC-MS, and NMR) with or without treatment with $NaBH_4$ as reported.[10] When required, the reaction was carried out with purging of the solution with argon for at least 30 min prior to addition of hydrogen peroxide and throughout the reaction course. Control experiments were carried out for all substrates under the same reaction conditions but without irradiation. In some experiments, *tert*-butyl alcohol at 100 or 200 mM was included in the oxidation mixture of **1**. In another experiment, oxidation of **1** (1 mM) was carried out with

(25) _Anslow, W. K.; Raistrick, H. *J. Chem. Soc.* **1939**, 1446−1454.
(26) Levy, G. C.; Lichter, R. L. *Nitrogen-15 Nuclear Magnetic Resonance Spectroscopy*; John Wiley & Sons: New York, 1979.
(27) Frisch, M. J.; Trucks, G. W.; Schlegel, H. B.; Scuseria, G. E.; Robb, M. A.; Cheeseman, J. R.; Zakrzewski, V. G.; Montgomery, J. A.; Stratmann, Jr. R.; Burant, E. J. C.; Dapprich, S.; Millam, J. M.; Daniels, A. D.; Kudin, K. N.; Strain, M. C.; Farkas, O.; Tomasi, J.; Barone, V.; Mennucci, B.; Cossi, M.; Adamo, C.; Jaramillo, J.; Cammi, R.; Pomelli, C.; Ochterski, J.; Petersson, G. A.; Ayala, P. Y.; Morokuma, K.; Salvador, P.; Dannenberg, J. J.; Malick, D. K.; Rabuck, A. D.; Raghavachari, K.; Foresman, J. B.; Ortiz, J. V.; Cui, Q.; Baboul, A. G.; Clifford, S.; Cioslowski, J.; Stefanov, B. B.; Liu, G.; Liashenko, A.; Piskorz, P.; Komaromi, I.; Gomperts, R.; Martin, R. L.; Fox, D. J.; Keith, T.; Al-Laham, M. A.; Peng, C. Y.; Nanayakkara, A.; Challacombe, M.; Gill, P. M. W.; Johnson, B.; Chen, W.; Wong, M. W.; Andres, J. L.; Gonzalez, C.; Head-Gordon, M.; Replogle, E. S.; Pople, J. A. *Gaussian 01*, Development Version (Revision A.01); Gaussian, Inc.: Pittsburgh, PA, 2001.

peroxidase (8.5 U/mL) and $H_2O_2$ (100 mM) and the reaction was halted by addition of catalase at various time intervals.

**Acknowledgment.** This work was carried out in the frame of the EC project "Ecotoxicological assessments and removal technologies for pharmaceuticals in wastewaters" REMPHARMAWATER (No EVK1-CT-2000-00048), and is also part of the research program "Tecniche Integrate di decontaminazione", sponsored by Regione Campania. GC-MS facilities were available at the Department of Chemical Engineering, University of Naples "Federico II". We thank the "Centro Interdipartimentale di Metodologie Chimico-Fisiche of Naples University for NMR facilities and Dr. Italo Giudicianni for technical assistance.

**Supporting Information Available:** $^{1}H$, $^{13}C$, $^{15}N$, $^{1}H,^{1}H$ COSY, $^{1}H,^{13}C$ HMQC/HMBC, and $^{1}H-^{15}N$ HMBC NMR spectra of the oxidation mixture of **1** in DMSO-$d_6$; MS data of main GC peaks and structural interpretation for nitrogenous species eluting under peaks 10, 14, 17, 18, 25, 26, 28, 30, 31, 33, and 35; and structures for recurrent and peculiar fragments of MS spectra. This material is available free of charge via the Internet at http://pubs.acs.org.

JO025604V